Materials & Design 211 (2021) 110135

Contents lists available at ScienceDirect

Materials & Design

journal homepage: www.elsevier.com/locate/matdes

Strain mapping of silicon carbon suspended membranes

Gerard Colston [a], Oliver Newell [a], Stephen D. Rhead [a], Vishal A. Shah [b], Maksym Myronov [a,*]

[a] Department of Physics, University of Warwick, Coventry, CV4 7AL, UK
[b] School of Engineering, University of Warwick, Coventry, CV4 7AL, UK

HIGHLIGHTS

- A novel process has been developed to fabricate suspended $Si_{1-y}C_y$ membranes.
- The process can be extended to silicon membranes as an alternative to SOI wafers.
- The strain of the suspended $Si_{1-y}C_y$ epilayer was measured using a μ -XRD technique.
- The tensile strain of the suspended $Si_{1-y}C_y$ increased by 20% of its original value.
- Increased tensile strain is caused by crystalline tilt at edges of the membrane.

GRAPHICAL ABSTRACT

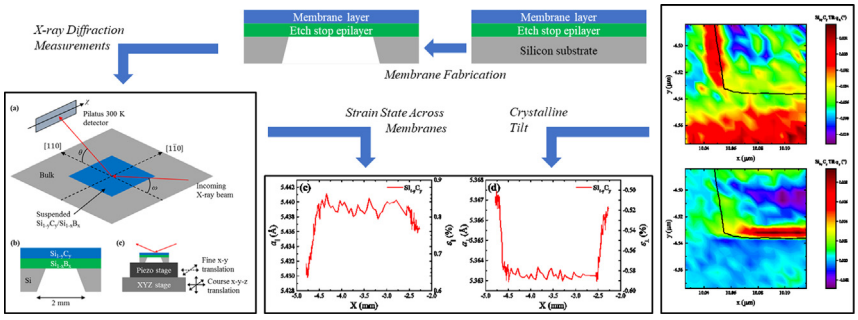

ARTICLE INFO

Article history:
Received 3 June 2021
Revised 24 September 2021
Accepted 27 September 2021
Available online 27 September 2021

Keywords:
Silicon carbon
Silicon boron
Strain
Membranes
MEMS

ABSTRACT

The alloy silicon carbon ($Si_{1-y}C_y$) has various strain engineering applications. It is often implemented as a dopant diffusion barrier and has been identified as a potential buffer layer for cubic silicon carbide (3C-SiC) heteroepitaxy. While suspended membranes formed from thin films of semiconductor (Ge and 3C-SiC) and dielectric (Si_3N_4) materials have been well studied, pseudomorphic, defect-free epilayers under high levels of tensile strain have received little attention. Often, tensile strain is a desired quality of semiconductors and enhancing this property can lead to various benefits of subsequent device applications. The strain state and crystalline tilt of suspended $Si_{1-y}C_y$ epilayers have been investigated through micro-X-ray diffraction techniques. The in-plane tensile strain of the alloy was found to increase from 0.67% to 0.82%. This strain increase could reduce the C content required to achieve suitable levels of strain in such alloys and further strain enhancement could be externally induced. The source of this strain increase was found to stem from slight tilts at the edges of the membranes, however, the bulk of the suspended films remained flat. The novel process utilised to fabricate suspended $Si_{1-y}C_y$ thin-films is applicable to many other materials that are typically not resistant to anisotropic Si wet etchants.

1. Introduction

Silicon carbon ($Si_{1-y}C_y$) is an alloy formed by the substitutional incorporation of C atoms into sites in the Si lattice and enables manipulation of the physical properties of the alloy from that of pure Si. The addition of C into the Si lattice changes the lattice constant according to the modified Vegard's Law [1] that approximately follows a linear interpolation between that of Si (y = 0) and cubic Silicon Carbide (3C-SiC) (y = 0.5). The resultant strain induced in $Si_{1-y}C_y$/Si heterostructures is around 10 times greater than the strain induced in $Si_{1-x}Ge_x$/Si heterostructures of equivalent substitutional composition. As a result, the main applications of $Si_{1-y}C_y$ alloys are found in strain engineering, such as inducing

* Corresponding author.
E-mail address: m.myronov@warwick.ac.uk (M. Myronov).

https://doi.org/10.1016/j.matdes.2021.110135
0264-1275/

strain within metal oxide semiconductor field effect transistor (MOSFET) channels to increase mobility [2] or compensating for the strain induced by Ge in $Si_{1-x-y}Ge_xC_y$ ternary alloys, such that the band structure can be modified whilst still matching the lattice structure of Si [3]. The incorporation of C in the Si lattice has also been shown to reduce "transient enhanced diffusion" [4]. This property has been utilized in various silicide applications such as increasing the maximum anneal temperature of Pt and Ni silicides [5,6] as well as reducing the Schottky barrier height with the aim to significantly reduce contact resistance [7]. One drawback to $Si_{1-y}C_y$ alloys is that it is very challenging to increase the C content of $Si_{1-y}C_y$ layers beyond around 1.5% without inducing significant densities of defects and amorphous inclusions during growth [8]. The only way around this issue is to use more reactive and expensive silicon and carbon based precursors or resort to non-conventional growth methods [9,10].

Another application for $Si_{1-y}C_y$ is as an intermediate epilayer for subsequent heteroepitaxy. One of the major issues when growing 3C-SiC directly on silicon substrates is the out diffusion of silicon into the growth of the 3C-SiC. This can lead to the formation of voids in the silicon at the interface which are one of the types of defects cosidered as device killers for power electronic applications and various efforts are made to reduce and eliminate their formation [11]. Growing on $Si_{1-y}C_y$ buffer layers can help to avoid this issue as the diffusion of material through $Si_{1-y}C_y$ is significantly reduced when compared to pure silicon, making $Si_{1-y}C_y$ alloys a potential buffer layer for 3C-SiC epitaxy [12,13]. In addition, $Si_{1-y}C_y$ has been shown to precipitate 3C-SiC at temperatures above 900 °C which could also help in subsequent nucleation of 3C-SiC on the surface [14].

Suspended membranes and microwires have already demonstrated various advantages over bulk material in Ge and SiGe alloys grown on Si such as reduced misfit dislocations, slight enhancements of tensile strain, improved optical properties as well as the potential for use as growth platforms for further epitaxy [15–18]. Suspending thin films is also a technique applied to 2-dimensional systems such as graphene, which have been formed into membranes for MEMS applications using novel processing techniques [19,20]. The fabrication of silicon membranes is extremely challenging as there is no distinction between epilayers and the substrates and suspended silicon is almost always achieved through the use of silicon-on-insulator (SOI) substrates [21]. Suspended membranes of thin (<100 nm) Si epilayers offer various applications for highly sensitive sensors, optical windows or compliant substrates, however, limitations with SOI substrates makes fabricating these structures difficult.

Suspending $Si_{1-y}C_y$ may offer a route to increasing tensile strain without relying on higher C content layers and could also act as suspended growth platforms for 3C-SiC. Heteroepitaxial growth on thin substrates has theoretically been shown to reduce the formation of defects and increase the critical thickness of pseudomorphic epilayers [22,23]. This is difficult to achieve in practise as the substrate thickness needs to be on the order of nanometers to have an impact on growth, however, this could be achieved through suspended films.

For $Si_{1-y}C_y$ membranes to be of use as growth platforms they must remain flat upon suspension, ideally without the edge effects that have previously been observed in suspended Ge and 3C-SiC membranes [24]. However, if these edge effects and inclusion of shear stresses are indeed the cause of tensile strain enhancements in suspended films, then these effects will be required for strain engineering purposes. In either case, the strain state and crystalline quality of suspended $Si_{1-y}C_y$ must be understood in order to determine its suitability for further practical applications.

$Si_{1-y}C_y$ alloys suffer from the same drawback as pure Si epilayers and are not resistant to standard Si etchants which makes it very dificult to fabricate suspended structures and membranes. To overcome this limitation, a novel fabrication process was developed through the introduction of an etch stop material that is compatible with standard silicon epitaxial processes and did not interfere with the epitaxial growth of the $Si_{1-y}C_y$ alloy and hence could also be utilised for the fabrication of suspended thin Si epilayers. This study aims to demonstrate the viability of fabricating $Si_{1-y}C_y$ membranes using this novel technique and dircetly measure the strain state and crystalline tilt of the alloy using an X-ray diffraction technique.

2. Experimental details

Unlike 3C-SiC and Ge, $Si_{1-y}C_y$ is not resistant to standard alkaline Si wet etchants such as potassium hydroxide (KOH) or tetramethylammonium hydroxide (TMAH) and therefore a suitable etch stop layer must be included in the heterostructure. Silicon boron ($Si_{1-x}B_x$) was chosen for this purpose as its lattice parameter reduces with increasing B content, as with $Si_{1-y}C_y$ and has been shown to resist the etching effect of TMAH [25]. $Si_{1-y}C_y$ layers were epitaxially grown on top of epitaxial $Si_{1-x}B_x$ layers on 100 mm diameter, 525 μm thick Si(001) substrates by reduced pressure chemical vapor deposition (RP-CVD) in an ASM Epsilon 2000 system. The $Si_{1-x}B_x$ layer was grown using diborane (B_2H_6) and disilane (Si_2H_6) precursors at 700 °C then immediately followed by the growth of the $Si_{1-y}C_y$ epilayers using disilane and trimethylsilane ($(CH_3)_3SiH$) precursors at 550 °C. The thickness of the $Si_{1-y}C_y$ epilayer was grown at ~ 20 nm as thinner epilayers have been shown to suffer from fewer surface defects [8]. To act as a suitable etch stop a slightly thicker $Si_{1-x}B_x$ layer was grown at ~ 50 nm. This technique could be used to suspend other epitaxial materials than are non-resistant to alkaline Si wet etchants including Si itself. Growing on a $Si_{1-x}B_x$ buffer offers an ideal etch stop layer for the fabrication of thin suspended Si membranes.

Lattice parameters of the heterostructures were collected using a lab based Panalytical X'Pert MRD diffractometer using Cu $K\alpha_1$ radiation. The in- and out-of-plane lattice parameters were determined by (224) and (004) reciprocal space maps (RSMs) respectively.

The suspended $Si_{1-y}C_y$ /$Si_{1-x}B_x$ membranes were fabricated in several stages [26]. A 2 mm × 2 mm window, over which the $Si_{1-y}C_y$/$Si_{1-x}B_x$ membrane was suspended, was first defined by optical lithography on the underside of the Si(001) substrate using an alkaline etch resistant ProTEK PSB photoresist. The $Si_{1-y}C_y$ surface was also protected by this photoresist. Then, the samples were etched in a 25 %wt. TMAH bath at 90 °C for approximately 16 h in order to etch through the entire Si substrate. The TMAH selectively etches the {001} Si planes whereas the {111} planes are etch resistant [27]. It is necessary to protect the $Si_{1-y}C_y$ layer as it is rapidly etched away in the TMAH bath. The fabrication of the suspended $Si_{1-y}C_y$ is only possible due to it being masked by the photoresist on the top side and the etch-resistant $Si_{1-x}B_x$ on the underside. The $Si_{1-y}C_y$ / $Si_{1-x}B_x$ membrane remains under tensile strain as it fixed to the $Si_{1-y}C_y$ / $Si_{1-x}B_x$ on Si (001) frame. Finally, the samples were treated in a Piranha etch (4:1, concentrated H_2SO_4 to 30 %wt·H_2O_2) for ~ 5 mins to remove the ProTEK photoresist followed by a 2.5 % HF dip for 30 s to remove any formed oxide on the $Si_{1-y}C_y$ surface.

Micro-diffraction experiments were performed on beamline B16 at the Diamond Light Source synchrotron [28] using X-rays with an energy of 14.6 keV (λ = 0.849 Å). A compound refractive lens was used to focus the X-ray beam with a spot size of approximately 4 μm × 4 μm. The sample was mounted on a piezo stage (50 nm precision) on top of an *XYZ* stage (0.5 μm precision) in a

fivecircle diffractometer allowing the sample to be moved through the beam, see Fig. 1.

Scattered X-rays were collected by a large PILATUS 300 K area detector capable of mapping the position of Bragg peaks in both 2θ (the scattering angle) and γ (the angle between the detector arm and the vertical plane). To locate the membrane, the diffractometer was aligned to the Si substrate (004) peak and the disappearance of this peak was observed as the sample was moved to a position where the beam only impinges on the suspended membrane without its Si substrate. The diffractometer was then aligned onto the $Si_{1-y}C_y$ (004) peak on the supported frame of the membrane and the detector centered on a scattering angle halfway between the Si substrate and $Si_{1-y}C_y$ layer peaks. The 2D slice acquired by the PILATUS detector for a given angle of incidence (ω) does not lie in the [001]-[1 1 0] plane in reciprocal space. Each column and row of pixels corresponds to a different 2θ and γ given by

$$2\theta = \text{atan}\left(\frac{w(p_m - p_i)}{L}\right) + 2\theta_m \gamma = \text{atan}\left(\frac{w(p_m - p_i)}{L}\right) + \gamma_m \quad (1)$$

where p_m is the middle pixel, p_i the index of the pixel in either the row or column, w = 172 μm and is the width of a single pixel, L is the distance from the sample to the detector (1.5 m) and $2\theta_m$ and γ_m are the angles the detector is centered on. Reciprocal space maps (RSMs) as a function of position were obtained across the sample by rocking ω around the (004) and (1 1 5) reflections at various spatial points. This set-up effectively gives us a 4D plot of measured intensity with respect to three variables (2θ, γ and ω). Fitting to these variables gives the position of the Bragg peaks in the coordinates of the diffractometer. For the case of the (004) RSMS it is possible to resolve the position of the Bragg peak in three axes q_x[110], $q_y\left[1\,\bar{1}\,0\right]$ and q_z[001] using

$$q_x = \frac{\lambda}{2}\sin(\theta)\sin(\omega - \theta) \quad (2)$$

$$q_y = \frac{\lambda}{2}\sin(\theta)\sin(\gamma) \quad (3)$$

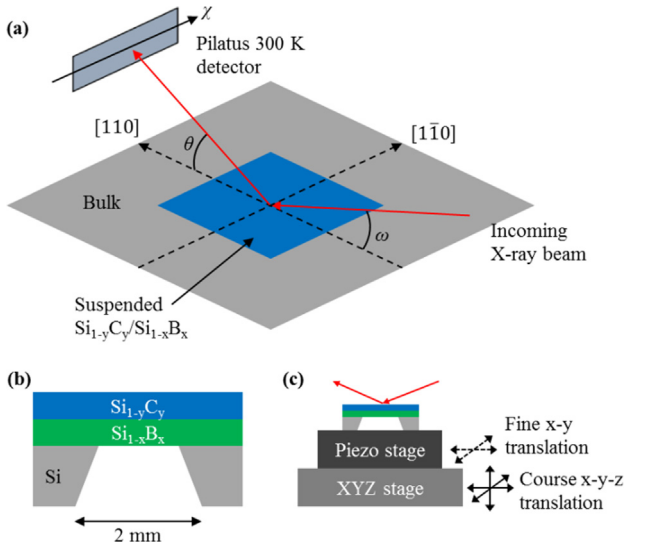

Fig. 1. (a) XRD scattering geometry for the acquisition of (004) RSMs. (b) Schematic cross-section of a 2 mm × 2 mm Si1-yCy/Si1-xBx membrane fabricated by selective wet etching. (c) Experimental set up of the fine translation piezo stage situated upon the course translation XYZ stage.

$$q_z = \frac{\lambda}{2}\sin(\theta)\cos(\omega - \theta) \quad (4)$$

where λ is the wavelength of the incident X-ray beam. This allows crystalline tilt to be measured in both in-plane directions of the sample surface by

$$tilt_{x/y} = \text{atan}\left(\frac{q_{x/y}}{q_z}\right)_{(004)} \quad (5)$$

The in-plane and out-of-plane lattice parameters of the crystal layers were calculated by taking RSMs around the $(1\,\bar{1}\,5)$ Bragg peak which was located by setting γ to 15.79° (the angle between the (004) and $(1\,\bar{1}\,5)$ planes) from the normal. In this case the in-plane and out-of-plane lattice parameters are defined by

$$q_{||} = \frac{\lambda}{2}\sin(\theta)\sin(\gamma - tilt_y) \quad (6)$$

$$q_{\perp} = \frac{\lambda}{2}\sin(\theta)\cos(\gamma - tilt_y) \quad (7)$$

respectively. This is only the case for these μ-XRD measurements as in order to get into the $(1\,\bar{1}\,5)$ Bragg diffraction condition the sample was rotated in γ to access the asymmetrical Bragg peak rather than in ω as with standard lab-based HR-XRD measurements.

Strain profiles for the suspended $Si_{1-x}B_x$ and $Si_{1-y}C_y$ were characterized by measuring symmetric (004) and asymmetric $\left(1\,\bar{1}\,5\right)$ RSMs every 10 μm along the $[1\,\bar{1}\,0]$ direction across the membrane edge along the middle of the sample. Once the edge was traversed the step size was increased to 25 μm along the membrane and subsequently reduced to 10 μm again as the other edge was approached to reduce the scan time. The membrane edge, incident and scattered X-rays were all parallel to the [1 1 0] direction of the crystal and the spatial resolution of the RSMs given by the spot size. The in- and out-of-plane lattice parameters ($a_{||}$ and $a_{\perp}$ respectively) were determined from the $(1\,\bar{1}\,5)$ RSMs after being corrected for the tilt measured from the (004) RSMs using

$$a_{||} = \frac{\sqrt{2}}{q_{||}}a_{\perp} = \frac{5}{q_{\perp}}. \quad (8)$$

The addition of the piezo stage allows fast maps to be generated; a 95 μm × 95 μm region is scanned in 6 μm increments for a given ω. Upon completion ω is incremented and the process repeated. This process continues until a ω is scanned across the Si, $Si_{1-x}B_x$ and $Si_{1-y}C_y$ (004) peaks. Once this area is mapped the *XYZ* stage is moved and the piezo scan repeated. Such a map can be obtained in approximately half the time compared to the generation of the same map from a series of line scans.

3. Results and discussions

A coupled scan shows that the inclusion of the $Si_{1-x}B_x$ buffer layer has little impact on the crystallinity of the $Si_{1-y}C_y$ epilayer as both (004) Bragg peaks can be seen from each layer, see Fig. 2. The broadness of the $Si_{1-y}C_y$ epilayer Bragg peak in the scan is a result of its low thickness. Thickness fringes can be seen in the plot also, however, the limited number of peaks visible makes it difficult to resolve the fringes due to each epilayer individually and cannot be used for thickness calibration. The presence of thickness fringes indicates that the epilayers are free from relaxation and any subsequent defect formation implying a high crystal qual-

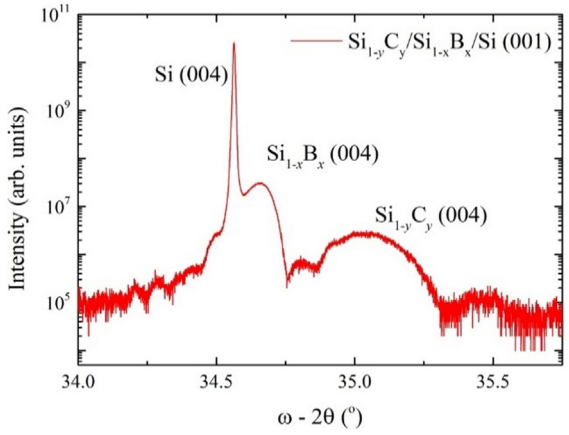

Fig. 2. ω-2θ coupled scan of the Si1-yCy/Si1-xBx/Si (001) heterostructure. Bragg peaks associated with each epilayer can be distinguished, the interference pattern of the thickness fringes resulting from each layer can also be seen.

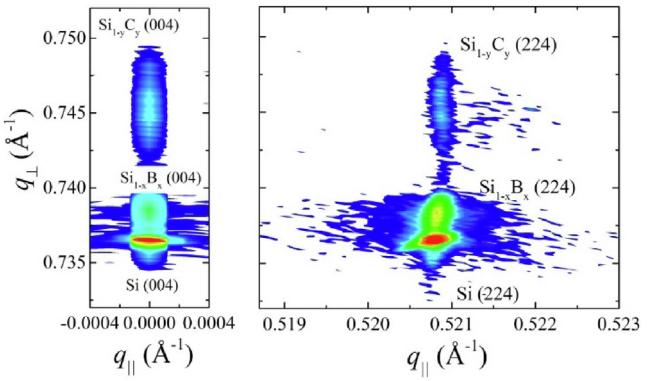

Fig. 3. Lab based RSMs around the (004) (left) and (224) (right) reflections. The $Si_{1-x}B_x$ and $Si_{1-y}C_y$ epilayers are tilt free and under 0.125% and 0.677% tensile strain respectively. The C content of the $Si_{1-y}C_y$ was calculated to be 1.5%.

ity. More experimental data highlighting the surface morphology and crystalline quality of $Si_{1-y}C_y$ epilayers grown using this technique can be found here [8].

Symmetric and asymmetric RSMs of the bulk grown materials were obtained using lab-based HR-XRD, see Fig. 3. The alignment of the (004) Bragg peaks indicate that both epilayers are free of tilt from the Si substrate. The strain state of the epilayers is determined from the positions of the tilt corrected (224) Bragg peaks. Both epilayers are found to be fully tensile strained to the Si substrate.

RSMs were collected at various spatial points across the suspended membrane using the 5-circle diffractometer collecting intensities across the 2D detector at a range of omega positions. This set-up effectively gives a 4D plot of measured intensity with respect to the three variables, see Fig. 4. Each variable was individually fit to using 1D Gaussians by projecting the data against the other two variables.

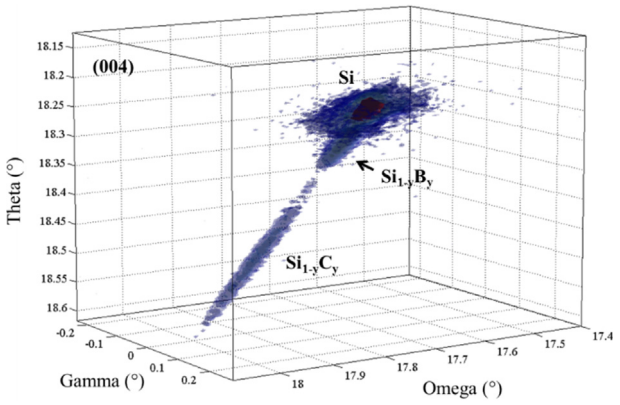

Fig. 4. 4D plot showing intensity *iso*-surfaces in the XRD measurement coordinates.

The strain profiles along the $[1\bar{1}0]$ direction across the suspended $Si_{1-x}B_x$ and $Si_{1-y}C_y$ are shown in Fig. 5.

An increase of in-plane tensile strain can be observed across both the $Si_{1-x}B_x$ and $Si_{1-y}C_y$ suspended epilayers of approximately $\Delta\varepsilon_{||} \approx 0.09\%$ and $\Delta\varepsilon_{||} \approx 0.15\%$ respectively, see Fig. 5 (a) ad (c). However, the uncertainty on these values is large due to nature of the in-plane calculations from the (1 1 5) reflection, see eq. (8), as such we will instead focus on the out-of-plane strain, which is inversely proportional to the in-plane strain assuming we have pure biaxial strain. This assumption will apply for the majority of the membrane and only becomes uncertain at the edges of the membrane. The out-of-plane lattice parameter contracts for the suspended $Si_{1-x}B_x$ and $Si_{1-y}C_y$ ($a_\perp$ = (5.4166 ± 0.0001) Å and (5.3633 ± 0.0002) Å) compared to the supported material ($a_\perp$ = (5.4192 ± 0.0002) Å and (5.3667 ± 0.0004) Å) resulting in the suspended material becoming more strained out-of-plane than the bulk material, see Fig. 5 (b) and (d). The reduction in the out-of-plane lattice parameter upon suspension is similar for both materials with $\Delta a_\perp \approx 0.003$ Å ($\Delta\varepsilon_\perp \approx 0.05\%$) although the uncertainties on the $Si_{1-y}C_y$ lattice constants are greater due to the reduced crystal quality and epilayer thickness. The out-of-plane strain is constant across the suspended structures with a very clear transition between the bulk and suspended material. This variation of strain is significantly more substantial that that observed in Ge suspended membranes [15].

The strain and tilt variations were mapped over a 2D area by performing a piezo scan across the corner of the membrane by the acquisition of (004) RSMs. In this case, the tilt refers to the variation of an epilayer crystal orientation with respect to itself. To make this possible, a reference point was taken upon the supported region of the structure and defined to have tilt equal to zero. Maps of $a_\perp$ for the suspended $Si_{1-x}B_x$ and $Si_{1-y}C_y$ are shown in Fig. 6.

As shown before in the linescan profiles, the out-of-plane lattice parameter is seen to decrease upon suspension from the silicon substrate. This implies that the in-plane lattice parameter has increased and as such the membrane is under more in-plane tensile strain. The area scans show no corner or edge effects in the strain variations of either the epilayers. Significantly more noise can be observed in the area map for the $Si_{1-y}C_y$ epilayer, however, the impact of suspension appears consistent between the $Si_{1-x}B_x$ and $Si_{1-y}C_y$ epilayers,

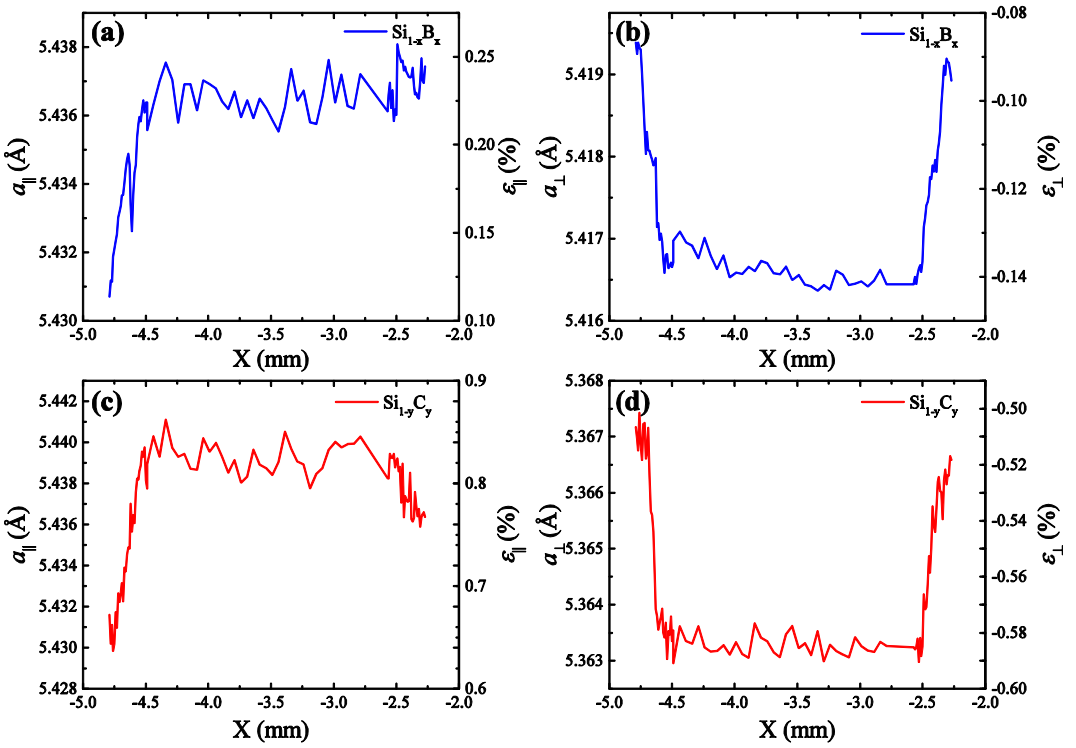

Fig. 5. The (a) $\varepsilon_{\parallel}$ and (b) $\varepsilon_{\perp}$ profiles across the suspended $Si_{1-x}B_x$ and (c) $\varepsilon_{\parallel}$ and (d) $\varepsilon_{\perp}$ profiles across the suspended $Si_{1-y}C_y$.

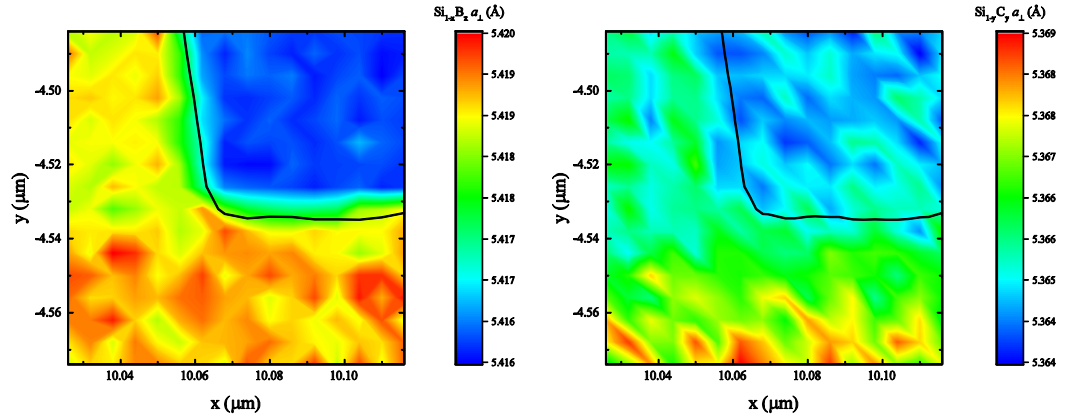

Fig. 6. 2-dimensional maps of the out-of-plane lattice parameters of the $Si_{1-x}B_x$ and $Si_{1-y}C_y$ suspended membrane corners. The boundary of the membrane is denoted by the black line and is defined by a decrease in the Si (004) Bragg peak intensity by 50%.

It had previously been suggested that tilt effects at the edge of suspended Ge and 3C-SiC membranes are the origin of this strain enhancement across the membrane entirety. In order to assess this explanation in more detail the tilt was calculated for the suspended membrane in both the q_x and q_y directions for both epilayers, see Fig. 7.

A significant increase in the tilt occurs along the borders of the membrane indicating the presence of shear strains along the membrane edges. These strains can account for the increase of in-plane lattice spacing found across the central region of the membrane which demonstrates biaxial strain. Similar effects can be observed in both epilayers, although there is significantly more noise in the variation of $a_{\perp}$ for the $Si_{1-y}C_y$ due to the epilayer being thinner. This indicates that the epilayers undergo the same physical distortions which are expected assuming the crystalline layers remain bound to one another. There is a slight misalignment between the positions of these tilt variations between the two epilayers; this is thought to be due to a slight shifting of the sample on the stage during the long measurement process.

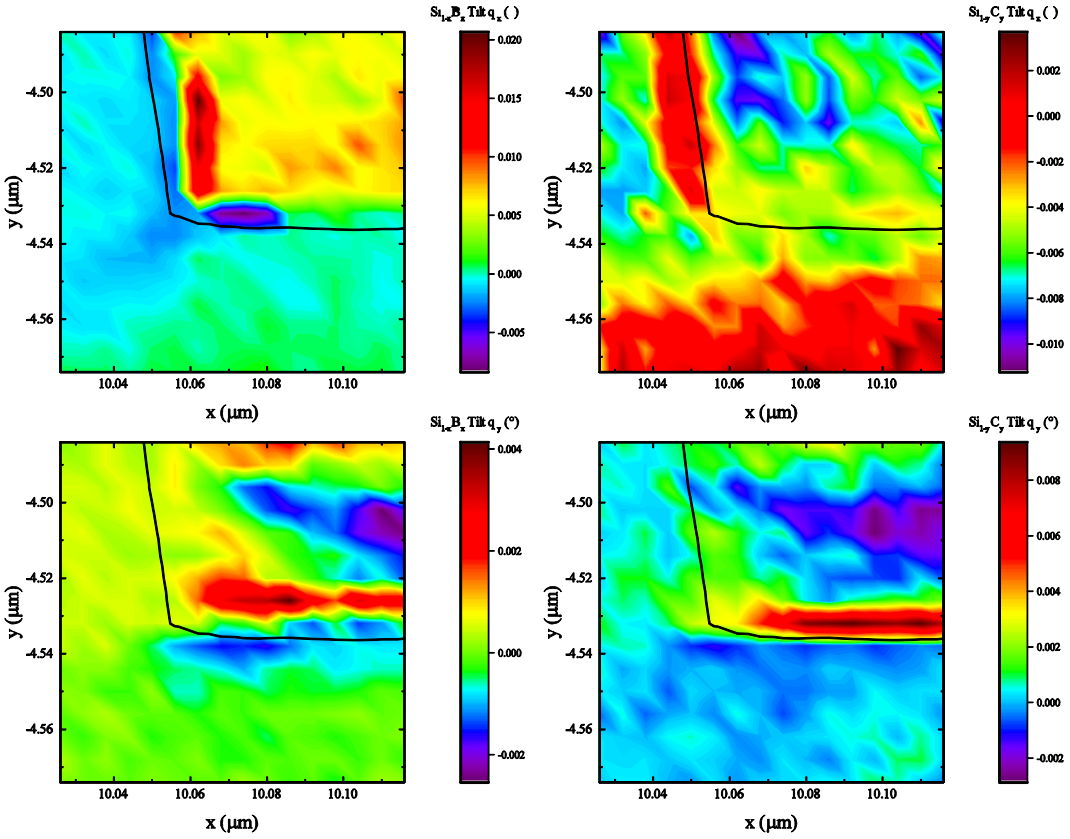

Fig. 7. 2-dimensional maps of the crystalline tilt, in both the q_x and q_y directions. In each case the tilt was defined as zero for the position at (10.03,-4.57). The boundary of the membrane is denoted by the black line and is defined by a decrease in the Si (004) Bragg peak intensity by 50%.

4. Conclusions

In other systems where strain has been measured across suspended semiconductor structures (Ge or 3C-SiC), the initial tensile strain has always been a residual effect from thermal expansion mismatch and upon suspension the increase or decrease of tensile strain has been a combination of relaxation from thermal mismatch and strain increase from shear stresses due to tilting of the epilayers. As the system measured here is under tensile strain due to lattice matching the $Si_{1-x}B_x$ and $Si_{1-y}C_y$ to the Si substrate, there is little impact of thermal mismatch.

The work presented here is the first example of strain mapping across a $Si_{1-y}C_y$ suspended structure and one of the first examples of a system under a high level of tensile strain. The fabricated membranes are found to remain intact after fabrication and can even undergo an aggressive piranha etch during the removal of a protective surface film. The process of suspending $Si_{1-y}C_y$ is shown to increase the in-plane strain of the system by approximately 1/5th of its original value (0.67% bulk to $\sim$ 0.82% suspended). This level of tensile strain in a $Si_{1-y}C_y$ epilayer is equivalent to a C content of $\sim$ 1.85%, using the modified Vegard's law this equates to an increase of 0.35% C from the epilayers actual composition of 1.5%. This increase in strain has been shown to be a result of the shear stresses and resulting tilt at the edges of the suspended membranes. While the increase in strain is modest it could be utilised to increase the performance of certain devices making use of a $Si_{1-y}C_y$ channel. A more ideal structure for this application could be with suspended $Si_{1-y}C_y$ wires which would not only restrict the current flow to certain dimensions but may further increase strain uniaxially in the direction of the current flow. Suspended membranes may be strained further by the presence of external stimuli such as physical force on the membrane or the creation of a pressure difference across the membrane, both of which would result in bowing and further tensile strain enhancement in the material. With the exception of edge effects, the membranes remain flat and therefore may present applications as compliant growth platforms for other materials, such as 3C-SiC. A novel membrane fabrication process was developed to overcome the lack of etch resistance of the $Si_{1-y}C_y$ alloy. The technique described, whereby a $Si_{1-x}B_x$ etch stop layer is employed, could be utilised in the fabrication of other suspended films including pure Si and offers a simple method of fabricating thin Si membranes on standard Si(001) substrates without relying on SOI wafers which often suffer from poor crystal quality, especially in thin (<100 nm) device layers.

In conclusion, micro-X-ray diffraction techniques have been used to map the strain and tilt variation across suspended bilayers of monocrystalline $Si_{1-x}B_x$ and $Si_{1-y}C_y$. An increase in tensile strain in both epilayers can be observed across the suspended square membrane of around a fifth of the initial strain in the bulk as-grown $Si_{1-y}C_y$ and $Si_{1-x}B_x$ epilayers. This strain variation is significantly more than in similar suspended m

Declaration of Competing Interest

The authors declare that they have no known competing financial interests or personal relationships that could have appeared to influence the work reported in this paper.

Acknowledgements

This research was supported by the EPSRC "Platform Grant" EP/J001074/1 and the STFC-funded MT11773 and MT10303 projects.

The Diamond Light Source is acknowledged for providing beamtime.

References

[1] P.C. Kelires, Short-range order, bulk moduli, and physical trends in c-Si1-xCx alloys, Phys. Rev. B 55 (1997) 8784.
[2] B.F. Hsieh, S.T. Chang, M.H. Lee, Characterization of silicon-carbon alloy materials for future strained Si metal oxide semiconductor field effect transistors, Thin Solid Films 529 (2013) 444.
[3] K. Eberl, S.S. Iyer, S. Zollner, J.C. Tsang, F.K. LeGoues, Growth and strain compensation effects in the ternary Si1−x−yGexCy alloy system, Appl. Phys. Lett. 60 (1992) 3033.
[4] P. Lavéant, G. Gerth, P. Werner, U. Gösele, Epitaxy of carbon-rich silicon with MBE, Mater. Sci. Eng. B 89 (2002) 241.
[5] K. De Keyser, B. De Schutter, C. Detavernier, V. Machkaoutsan, M. Bauer, S.G. Thomas, J. Jordan Sweet, C. Lavoie, Phase formation and texture of nickel silicides on Si1−xCx epilayers, Microelectron. Eng. 88 (2011) 536.
[6] K.R. Lee, I.P. Lin, H.T. Chang, S.W. Lee, Platinum silicide formation on Si1-yCy epitaxial layers, J. Alloy. Compd. 574 (2013) 415.
[7] P.S.Y. Lim, R.T.P. Lee, M. Sinha, D.Z. Chi, Y.C. Yeo, Effect of substitutional carbon concentration on Schottky-barrier height of nickel silicide formed on epitaxial silicon-carbon films, J. Appl. Phys. 106 (2009) 5.
[8] G. Colston, M. Myronov, S. Rhead, D. Leadley, Analysis of surface defects in Si1−yCy epilayers formed by the oversaturation of carbon, Semicond. Sci. Technol. 30 (2015) 114003.
[9] M. Bauer, V. Machkaoutsan, C. Arena, Highly tensile strained silicon-carbon alloys epitaxially grown into recessed source drain areas of NMOS devices, Semicond. Sci. Technol. 22 (1) (2007) S183–S187.
[10] A. Gouye, O. Kermarrec, A. Halimaoui, Y. Campidelli, D. Rouchon, M. Burdin, P. Holliger, D. Bensahel, Low-temperature RPCVD of Si, SiGe alloy, and Si1-yCy films on Si substrates using trisilane (Silcore (R)), J. Cryst. Growth 311 (2009) 3522.
[11] F. La Via, A. Severino, R. Anzalone, C. Bongiorno, G. Litrico, M. Mauceri, M. Schoeler, P. Schuh, P. Wellmann, From thin film to bulk 3C-SiC growth: Understanding the mechanism of defects reduction, Mater. Sci. Semicond. Process. 78 (2018) 57–68.
[12] H. Nakazawa, M. Suemitsu, Low-temperature formation of an interfacial buffer layer using monomethylsilane for 3C-SiC/Si(100) heteroepitaxy, Appl. Phys. Lett. 79 (2001) 755.
[13] G. Colston, M. Myronov, Electrical properties of n-type 3C-SiC epilayers in situ doped with extremely high levels of phosphorus, Semicond. Sci. Technol. 33 (2018) 114007.
[14] C. Guedj, M.W. Dashiell, L. Kulik, J. Kolodzey, A. Hairie, Precipitation of beta-SiC in Si1-yCy alloys, J. Appl. Phys. 84 (1998) 4631.
[15] S.D. Rhead, J.E. Halpin, V.A. Shah, M. Myronov, D.H. Patchett, P.S. Allred, V. Kachkanov, I.P. Dolbnya, J.S. Reparaz, N.R. Wilson, C.M.S. Torres, D.R. Leadley, Tensile strain mapping in flat germanium membranes, Appl. Phys. Lett. 104 (2014) 5.
[16] V.A. Shah, S.D. Rhead, J.E. Halpin, O. Trushkevych, E. Chavez-Angel, A. Shchepetov, V. Kachkanov, N.R. Wilson, M. Myronov, J.S. Reparaz, R.S. Edwards, M.R. Wagner, F. Alzina, I.P. Dolbnya, D.H. Patchett, P.S. Allred, M.J. Prest, P.M. Gammon, M. Prunnila, T.E. Whall, E.H.C. Parker, C.M.S. Torres, D.R. Leadley, High quality single crystal Ge nano-membranes for opto-electronic integrated circuitry, J. Appl. Phys. 115 (2014) 10.
[17] J. Gao, J. Sun, J. Jiang, Y.i. Zhang, Demonstration of biaxially tensile-strained Ge/SiGe multiple quantum well (MQW) electroabsorption modulators with low polarization dependence, Nanophotonics 9 (2020) 4355.
[18] L.Q. Zhou, G. Colston, M. Myronov, D.R. Leadley, O. Trushkevych, V. Shah, R.S. Edwards, Ultrasonic Inspection and Self-Healing of Ge and 3C-SiC Semiconductor Membranes, J. Microelectromech. Syst. 29 (2020) 370.
[19] Xuge Fan, Anderson D. Smith, Fredrik Forsberg, Stefan Wagner, Stephan Schröder, Sayedeh Shirin Afyouni Akbari, Andreas C. Fischer, Luis Guillermo Villanueva, Mikael Östling, Max C. Lemme, and Frank Niklaus, Manufacture and characterization of graphene membranes with suspended silicon proof masses for MEMS and NEMS applications, Microsyst. Nanoeng. 6 (2020) 17.
[20] Shirin Afyouni Akbari, Vahid Ghafarinia, Tom Larsen, Marsha M. Parmar, and Luis Guillermo Villanueva, Large Suspended Monolayer and Bilayer Graphene Membranes with Diameter up to 750 μm, Sci. Rep. 10 (2020) 6426.
[21] A. Varpula, A.V. Timofeev, A. Shchepetov, K. Grigoras, J.h. Hassel, J. Ahopelto, M. Ylilammi, M. Prunnila, Thermoelectric thermal detectors based on ultra-thin heavily doped single-crystal silicon membranes, Appl. Phys. Lett. 110 (2017) 262101.
[22] Y.H. Lo, New approach to grow pseudomorphic structures over the critical thickness, Appl. Phys. Lett. 59 (1991) 2311.
[23] Y. Song, K. Wang, D.u. Pengwei, Z. Cheng, Suspended-ultrathin Si membrane on SOI: a novel structure to reduce thermal stress of GaN epilayer, IOP Conference Series: Materials Science and Engineering 768 (2020) 022053.
[24] G. Colston, S.D. Rhead, V.A. Shah, O.J. Newell, I.P. Dolbnya, D.R. Leadley, M. Myronov, Mapping the strain and tilt of a suspended 3C-SiC membrane through micro X-ray diffraction, Mater. Des. 103 (2016) 244.
[25] E. Steinsland, M. Nese, A. Hanneborg, R.W. Bernstein, H. Sandmo, G. Kittilsland, Boron etch-stop in TMAH solutions, Sensors Actuators a-Phys. 54 (1996) 728.
[26] V.A. Shah, M. Myronov, C. Wongwanitwatana, L. Bawden, M.J. Prest, J.S. Richardson-Bullock, S. Rhead, E.H.C. Parker, T.E. Whall, D.R. Leadley, Electrical isolation of dislocations in Ge layers on Si(001) substrates through CMOS-compatible suspended structures, Sci. Technol. Adv. Mater. 13 (2012) 7.
[27] O. Tabata, R. Asahi, H. Funabashi, K. Shimaoka, S. Sugiyama, Anisotropic etching of silicon in TMAH solutions, Sens. Actuators, A 34 (1992) 51.
[28] K.J.S. Sawhney, I.P. Dolbnya, M.K. Tiwari, L. Alianelli, S.M. Scott, G.M. Preece, U. K. Pedersen, R.D. Walton, A Test Beamline on Diamond Light Source, AIP Conf. Proc. 1234 (2010) 387.